Dynamic Response Analysis of High Voltage Transmission Tower-Line Coupling System Under Ice and Wind Loads

Bingzhao Qiu
College of Mechanical and Electrical Engineering
Northeast Forestry University
Harbin, China
qiubingzhao@126.com

Mingfei Ban*
College of Computer and Control Engineering
Northeast Forestry University
Harbin, China
banmingfei@nefu.edu.cn

Yiqi Liu
College of Computer and Control Engineering
Northeast Forestry University
Harbin, China
liuyq0925@126.com

Long Dai
College of Computer and Control Engineering
Northeast Forestry University
Harbin, China
dailong1853@163.com

2024 4th Power System and Green Energy Conference (PSGEC) | 979-8-3503-6557-3/24/$31.00 ©2024 IEEE | DOI: 10.1109/PSGEC62376.2024.10721088

***Abstract*—Investigating the dynamic characteristics of high-voltage (HV) transmission line coupling systems under ice-wind loads is crucial for bolstering the system's resilience to ice and snow disasters, thereby ensuring power supply safety. Currently, developing an effective analysis method is a focal point in this research domain. This study selects a representative HV transmission line as the subject of investigation and constructs an ice-wind loads coupling model. Using the 220kV ice-covered HV transmission line of the Fujian power grid as a case study, the comprehensive effects of ice thickness, wind attack angle and speed are considered based on the coupled finite element model (FEM). The response characteristics of the HV transmission line ice-wind loads are analyzed, and key parameters such as stress response and displacement response are evaluated. The findings indicate that the ice-wind response of the tower-line system can be effectively analyzed. The simulation calculation model of the transmission line under the tower-line coupling factors presented in this paper aligns more closely with actual working conditions, making it a valuable reference for the design, mechanical analysis, and operation and maintenance of HV transmission lines in specific regions.**

***Index Terms*—HV transmission line, tower-line coupling system, ice-wind loads, dynamic response, FEM**

I. Introduction

The reliability of power system is intrinsically tied to the integrity and dependability of HV transmission lines, which are crucial in ensuring a secure power supply [1]. In regions prone to prolonged low temperatures and high humidity during winter, HV transmission lines are particularly susceptible to the effects of ice-wind loads, which alter their original load-bearing characteristics and mechanical distribution. Severe conditions can lead to permanent deformation of tower structures, wire breakage, and tower collapse, resulting in widespread power outages [2], [3]. China's varied topography and complex climate lead to regional differences in the probabilistic distribution of wind speeds and ice thickness [4]. Ice-related incidents on HV transmission lines are characterized by extensive impact, prolonged duration, and challenging repair efforts, posing significant threats to grid reliability [5]. Consequently, it is crucial to study the system characteristics of transmission line when subjected to the combined impacts of ice-wind loads. This involves a precise analysis of their bearing performance under these conditions, an understanding of the distribution of potential weak points, and the ability to predict the types and likelihood of accidents in various scenarios. This research is essential for optimizing anti-icing design, operation, maintenance, and de-icing strategies.

To mitigate the adverse effects of ice and wind loads on transmission tower-line systems, scholars both domestically and internationally have conducted a series of studies on their response patterns. These studies include theoretical derivation [6], field measurements [7], full-scale or scaled physical model experiments [8], and finite element analysis [9]. To improve the accuracy of predicting and evaluating the response of transmission line under ice-wind loads, numerical simulation techniques based on finite element theory have gained prominence. This preference is largely due to their superior precision, cost-effectiveness, and streamlined parameter configurations [10]. Reference [11] studied the system characteristics of transmission line structures utilizing numerical simulation methodologies. In reference [12], ANSYS software was used to model a 1220m long-span transmission system across the Songhua River to analyze wind-induced vibration problems.

This work was supported by the National Natural Science Foundation of China (52107075), the Fundamental Research Funds for the Central Universities (2572024AW10). *Corresponding author: Mingfei Ban.*

Reference [13] presented a model specifically developed to analyze line jumps in engineering, with a particular focus on determining the dynamic approach distance of lines under both uniform and non-uniform icing and de-icing conditions. The study scrutinized the longitudinal unbalanced tension values of typical HV lines under de-icing jump conditions to ensure their safe operation. Reference [14] studied the jumping behavior of ice-covered lines, formulated the tower self-vibration model, and employed numerical simulation to investigate the jumping characteristics of icing lines. This study introduced an efficient method for forecasting the wind speed's jumping range. Reference [15] researched the bearing performance of transmission towers under varying ice thickness and wind attack angles, discovering that the materials of the tower body significantly influence overall stability under ice and wind loads.

Comparing these research findings reveals that current studies on HV transmission tower-line systems primarily focus on analyzing icing characteristics, types, and wind field features. There is a notable absence of a comprehensive study examining the mechanical properties and dynamic characteristics of HV transmission line when subjected to the combined effects of ice-wind loads in specific regions. Consequently, the research gap persists in examining the mechanical properties and dynamic characteristics of HV tower-line systems under various conditions.

To highlight the impact of HV transmission line coupling effects on the mechanical properties of tower-line systems under ice-wind loads, this paper first discusses the consideration of tower-line coupling factors in finite element simulation methods, combined with mathematical models. Subsequently, a 220kV HV transmission line in an iced area within the Fujian power grid is used as a case study. The modeling simulation of the HV transmission line system is completed, considering the local climatic characteristics, and key indicators such as the stress distribution of transmission towers, conductors, and ground wires, as well as the ultimate ice thickness and wind speed, are solved. The response characteristics of transmission lines are determined by comparing the index differences associated with varying wind attack angles, wind speeds, and ice thicknesses. The findings underscore the necessity of incorporating the coupling factors of tower lines into the mechanical analysis of these structures when subjected to ice-wind loads. This research offers a significant reference for strategically placing monitoring terminals on HV transmission lines.

II. FEM FOR HV TRANSMISSION LINE TOWER-LINE COUPLING SYSTEM

Transmission lines are intricate, interconnected structures composed of towers, conductors, ground wires, insulator strings, and fittings. Utilizing the ANSYS finite element development environment allows for the creation of a highly detailed FEM that accurately represents the actual structure.

A. Transmission Tower Modeling

Transmission towers represent quintessential spatial truss structures, amenable to analysis through the finite element method [16]. The mass matrix S_e^n and stiffness matrix T_e^n of the nth unit, as defined in the local coordinate system, are transformed into matrices within the global coordinate system utilizing a specific transformation matrix R_m^n.

$$\begin{cases} \bar{S}_e^n = \left(R_m^n\right)^{\mathrm{T}} S_e^n R_m^n \\ \bar{T}_e^n = \left(R_m^n\right)^{\mathrm{T}} T_e^n R_m^n \end{cases} \tag{1}$$

where $\bar{S}_e^n$ and $\bar{T}_e^n$ are the mass and stiffness matrices in the global coordinate system, respectively.

Moreover, the comprehensive mass matrix T_t and stiffness matrix S_t of the transmission line tower structure are derived by amalgamating each unit.

$$\begin{cases} T_t = \sum\limits_{n=1}^{me} \left(R_c^n\right)^{\mathrm{T}} \bar{T}_e^n R_c^n \\ S_t = \sum\limits_{n=1}^{me} \left(R_c^n\right)^{\mathrm{T}} \bar{S}_e^n R_c^n \end{cases} \tag{2}$$

where me represents the total number of cells in the transmission tower; R_c^n is the degree-of-freedom localization matrix.

Transmission towers provide essential structural support for components such as overhead lines, insulators, and metal fittings, ensuring reliable insulation of the overhead lines. To accurately simulate the tower's actual stress conditions, including tower body inclination and bending moments on the primary tower leg materials, a hybrid truss model is employed for tower modeling. The Beam188 element is used to model the diagonal and cross-bracing members of transmission towers. Various material properties are defined to replicate the angle steel used in the tower's construction, with connections rigidly set. The Link8 element is selected to simulate auxiliary materials.

B. Overhead Line Modeling

As illustrated in Fig.1, overhead lines primarily adopt a suspension structure and exhibit a catenary shape under their weight. To accurately replicate the catenary characteristics of these overhead lines, this paper employs Link10 elements to capture their flexible properties.

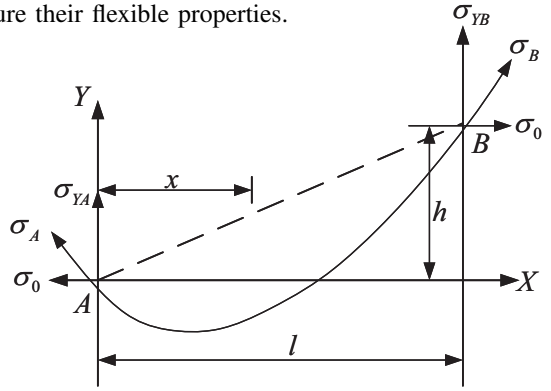

Fig. 1. Catenary model of overhead line

The Irvine system predominantly concentrates on the vibrational attributes of catenaries, with its research outcomes frequently employed as theoretical analytical solutions to evaluate their performance [17]. The formulas and models for catenaries are delineated below.

$$\begin{cases} y = \frac{\varepsilon}{L_{\varepsilon=0}} \left[\frac{2\sigma_0}{\gamma} \mathrm{sh} \frac{\gamma x}{2\sigma_0} \mathrm{ch} \frac{\gamma(l-x)}{2\sigma_0} \right] - \Xi \\ \Xi = \sqrt{1 + \left(\frac{\varepsilon}{L_{\varepsilon=0}} \right)^2} \cdot \frac{2\sigma_0}{\gamma} \mathrm{sh} \frac{\gamma x}{2\sigma_0} \mathrm{ch} \frac{\gamma(l-x)}{2\sigma_0} \end{cases} \tag{3}$$

$$L_{\varepsilon=0} = \frac{2\sigma_0}{\gamma} \mathrm{sh} \frac{\gamma l}{2\sigma_0} \tag{4}$$

where ε is the height difference between the suspension points at both ends of the overhead line, m; $L_{h=0}$ is the catenary length of overhead lines at equal heights, m; γ represents the wire ratio load, $\mathrm{MPa.m^{-1}}$; σ_0 represents the axial stress at the nadir of the sag, MPa; l is the overhead line span, m.

C. Insulators and Fittings Modeling

Insulators are crucial components that bridge the gap between the wire and the transmission tower, ensuring essential electrical insulation. The insulator string of the line can be conceptualized as a rigid rod, modeled using the Link8 element in finite element analysis. This rod is hinged at its points of connection with both the transmission tower and the wire.

Fittings are typically modeled using beam elements. However, in existing studies, it can be represented either by rod elements or cable elements.The stiffness matrix K_{SC} can be articulated as follows:

$$K_{SC} = \sum_{i=1}^{nc} K_C^i + \sum_{j=1}^{nb} K_{BR}^j \tag{5}$$

where nc represents the quantity of split conductors; nb represents the quantity of fittings; K_C is the stiffness matrix of a single wire; K_{BR} is the stiffness matrix of fittings.

III. Analytical Modeling and Computation of Tower-Line Coupling System

A. Nonlinear Equations for Tower-Line System

This paper employs an analytical approach to identify three pivotal parameters: stress along the overhead line, ice thickness, and varying winds. It accounts for the coupling and non-linearity inherent in the tower-line system, subsequently providing a comprehensive equilibrium equation [18].

$$\left([K_E] + [K_G] + [K_{NL}]\right)\{\Theta\} = \{\mathrm{X}_0\} + \{\mathrm{X}\} + \{R\} \tag{6}$$

where K_E, K_G represent the overall elastic stiffness matrix and geometric stiffness matrix, respectively; K_{NL} is the initial displacement matrix; Θ is the displacement vector of the nodes in the system that needs to be studied; X_0 is the initial force vector; X is the unbalanced force vector; R is the load vector of the node.

The Newton-Raphson equilibrium iteration method is adept at resolving the aforementioned nonlinear equations, thereby ensuring that the solutions attained after each load exhibit robust balance convergence.

B. Computation Method for Tower-Line Coupling System

(1) Stress along the overhead line

A prevalent assumption in engineering posits that the load per unit length of a conductor is distributed uniformly. This assumption facilitates the derivation of the stress-sag relationship as outlined below.

$$f_m = \frac{\gamma l^2}{8\sigma_0 \cos\beta} \tag{7}$$

where f_m is the sag of the conductor, m; β is the angle of elevation.

The axial force experienced along the line of transmission lines in the tension section can be determined by examining the correlation between this axial force and the lowest point axial force. The precise calculation method is as follows:

$$\begin{cases} \sigma_x = \frac{\sigma_0}{\cos\beta} + \gamma \left[x \tan\beta - \frac{\gamma x(l-x)}{2\sigma_0 \cos\beta} \right] - \Delta \\ \Delta = \gamma \left(\frac{l}{2} \tan\beta - \frac{\gamma l^2}{2\sigma_0 \cos\beta} \right) \end{cases} \tag{8}$$

where σ_x represents the axial force along the overhead line, MPa ; x is the coordinate along the overhead line, m.

(2) Ice-load

In the computation of overhead lines, the load ratio is characterized as the load value per unit length and per unit cross-sectional area. The self-weight load ratio χ_1 and ice-weight load ratio χ_2 of the conductor are detailed below.

$$\begin{cases} \chi_1 = \frac{qg}{A} \times 10^{-3} \\ \chi_2 = 27.728 \frac{b(d+b)}{A} \times 10^{-3} \end{cases} \tag{9}$$

where q denotes the mass of the conductor per kilometer, kg/m; A signifies the cross-sectional area of the conductor, $\mathrm{mm^2}$; b represents the thickness of the ice coating, mm; d indicates the outer diameter of the conductor, mm.

The vertical load ratio χ of the conductor is determined by the cumulative effect of both the self-weight load ratio and the ice-weight load ratio.

(3) Wind-load

This paper acknowledges both static and dynamic wind loads as integral components of the total wind load. The formula utilized to calculate the wind load exerted on a unit area of the towering structure is delineated below.

$$\begin{cases} W_s = \mu_z \mu_s \beta_z B A_f W_0 \\ W_0 = \frac{v^2}{1600} \end{cases} \tag{10}$$

where μ_z is the variation coefficient of wind pressure height; μ_s denotes the shape factor of the component; β_z is the adjustment coefficient; B signifies the increased coefficient of wind load when covered with ice; A_f is the projected area under wind pressure, $\mathrm{mm^2}$; W_0 is the standard value of reference wind pressure, $\mathrm{N/m^2}$; v is wind speed, $\mathrm{m/s}$.

IV. Example Results and Analysis

This paper investigates a representative 220kV overhead transmission line within the Fujian power grid. Situated in a mountainous region with intricate terrain, cold winter temperatures, and frequent winds, this line is prone to ice accretion

and high-wind events. The tension section between towers 97 and 98 has been selected for this study, with its mechanical schematic illustrated in Fig.2. Tower number 97, referred to as the wine glass tower, is located at the highest elevation of this segment and demonstrates a significant span and height disparity compared to the adjacent tension towers. The left and right spans measure 229m and 309m, respectively, with height differences of 47m and 80m from the neighboring towers.

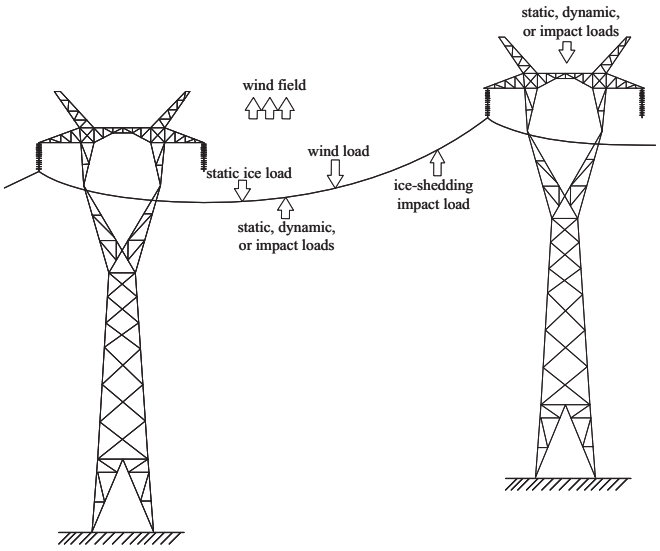

Fig. 2. Mechanical diagram of HV transmission line (ice-wind loads)

A. Stress-Strain Analysis of Tower-Line Coupling System

Considering the severe climatic conditions, FEM of the two towers and three lines system was established using ANSYS simulation software. This paper conducted simulations under

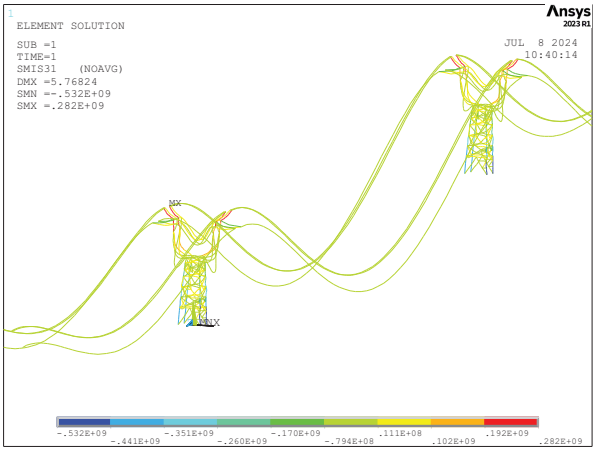

Fig. 3. Strain state diagram of the tower-line system (axial stress)

49 combinations of ice-wind loads (ice thickness d=0mm, 10mm, 20mm, 30mm, 40mm, 50mm, 60mm; wind speed v=5m/s, 10m/s, 15m/s, 20m/s, 25m/s, 30m/s, 35m/s). The simulation results for the HV transmission line model under the conditions of 30mm ice thickness and wind speed of

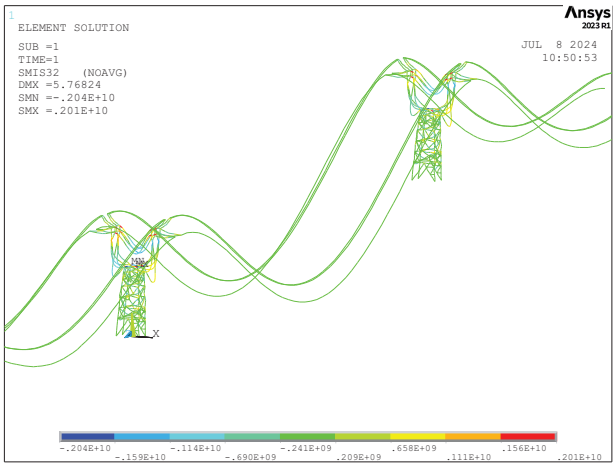

Fig. 4. Strain state diagram of the tower-line system (bending stress)

15m/s were selected, producing axial and bending stresses, as shown in Fig.3 and Fig.4, respectively.

Furthermore, an analysis was conducted on the mechanical properties of HV transmission line systems under varying ice thicknesses. The stress distribution values, including axial and bending stress, were documented for different ice thicknesses. The pattern of stress variation within the system was subsequently analyzed, as depicted in Fig.5.

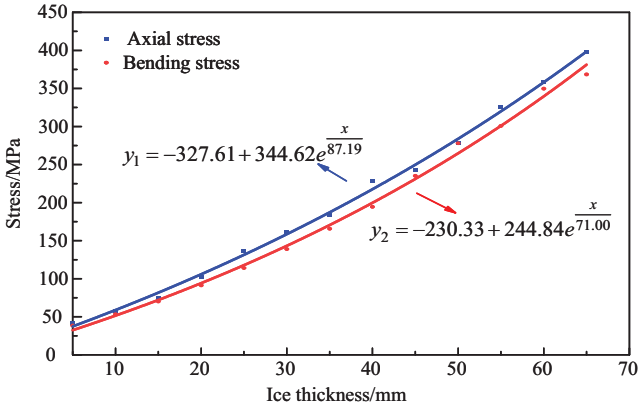

Fig. 5. Stress-ice thickness variation curve

1) As the ice thickness on the tower-line system continues to increase, the axial stress and bending stress experienced by the tower components also increase.

2) The functions y_1 and y_2 are respectively the fitting functions for axial stress and bending stress, with a fitting degree reaching above 0.98.

3) When the ice thickness reaches 60mm, the maximum axial stress value that the tower components can bear is approximately 358.2MPa, and the maximum bending stress value is approximately 349.7MPa, both of which exceed the allowable stress of 345MPa (the material of angle steel is Q345), causing damage to the components.

B. Dynamic Response of Tower-Line Coupling System

The displacement responses of each section point of the transmission tower under various working conditions were

extracted based on the analysis results. Fig.6 illustrates the diagram defining the wind attack angle, along with the specific positions and numbers of nodes. Nodes NO.719 and NO.895 represent the top points of the grounding wire bracket, while nodes NO.583 and NO.652 denote the midpoints at the ends of the crossbeam.

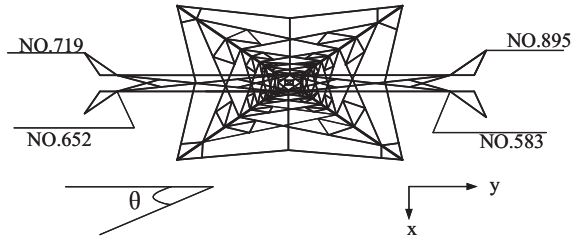

Fig. 6. Schematic diagram of node position and wind attack angle θ

(1) Various wind speeds

To more thoroughly investigate the influence of wind speed on displacement in all directions within the ice-covered tower line system, maximum displacement responses in all directions at varying wind speeds for each node were extracted. Subsequently, a wind speed-maximum displacement curve, as depicted in Fig.7, was plotted.(d= 30mm, θ =0°)

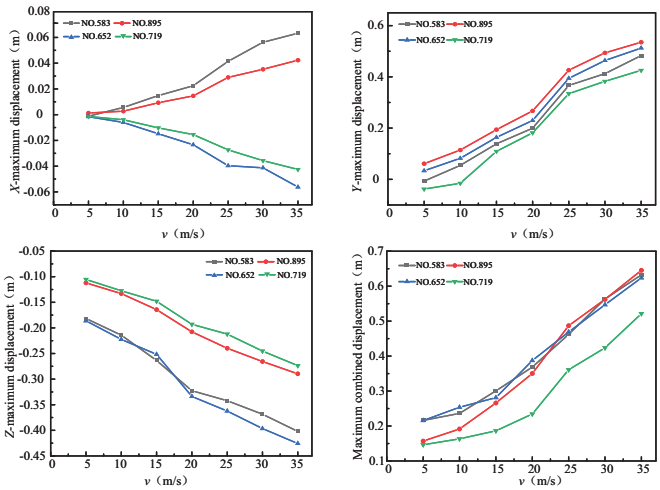

Fig. 7. Wind speed-maximum displacement curve

1) The maximum displacement in all directions of the nodes within the HV transmission line system is observed at a wind speed of 35m/s, corresponding to a typhoon.

2) An upward trend in the curve indicates that the displacement response of the transmission tower nodes increases proportionally with wind speed.

3) Among all directional maximum displacement values of the nodes, the most pronounced responses occur in the Y-direction and Z-direction, aligning with the direction of the ice-wind loads.

(2) Various wind attack angles

In standard conditions, the wind attack angle is a critical parameter in defining the response characteristics of HV transmission lines. According to the IEC international standard, θ =0°, 60° are generally deemed least favorable for tower operation.By setting a wind speed of v= 15m/s and an ice thickness of d= 30mm, we collected displacement time-history response data from various nodes of the tower at wind attack angles of θ =0°, 30°, 45°, 60°, 90°. This facilitates our examination of the most detrimental wind attack angle for HV transmission lines. It also enables us to scrutinize the influence of the wind attack angle on the displacement response in various system directions and to extract the maximum displacement of both the tower ground wire bracket and crossarm end nodes, as depicted in Fig.8.

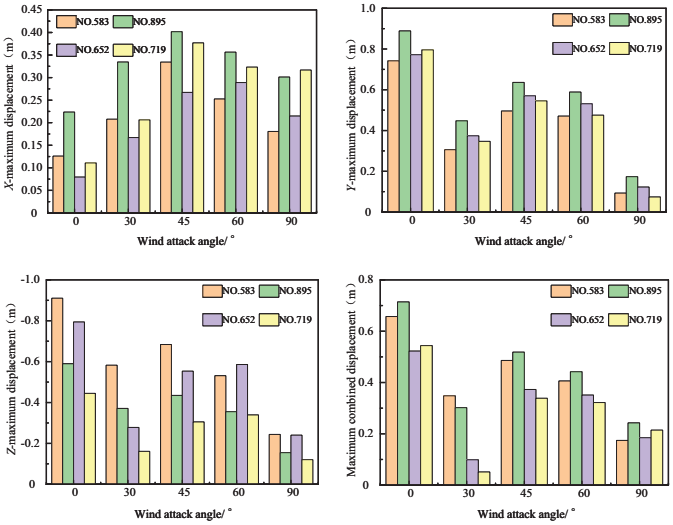

Fig. 8. Wind attack angle-maximum displacement curve

1) The peak displacement in the X-direction is observed at a wind attack angle of θ = 45°, with the most significant displacement node located at the apex of the grounding support.

2) The peak displacement in the Y-direction is observed at a wind attack angle of θ =0°, with the most significant displacement node located at the apex of the grounding support.

3) The peak displacement in the Z-direction is observed at a wind attack angle of θ =0°, with the node of maximum displacement situated at the midpoint of the crossbeam's end.

4) The peak combined displacement occurs at a wind attack angle θ =0°. On the leeward side, the response pattern for combined displacement is as follows: 0°> 45°> 60°> 30°> 90°. Conversely, on the windward side, the sequence is 0° > 45° > 60° > 90° > 30°. A wind attack angle of 0° is deemed the least favorable.

V. Conclusion

This paper examines the FEM for simulating ice-wind loads and its associated calculations, with a particular emphasis on the tower-line coupling effect. We utilize practical engineering data to select a specific line of the Fujian power grid as a case study to analyze the response characteristics of HV transmission lines under ice-wind loads. Our research investigates the impact of parameters such as ice thickness, wind attack angle and speed on the dynamic behavior of the system. Upon

reviewing the aforementioned analysis and discussion, we can deduce the following conclusions.

1) The investigation into the dynamic characteristics of transmission lines in Fujian's power grid under combined ice-wind loads reveals that, with a constant ice layer thickness, an increase in wind speed results in enhanced dynamic response. Conversely, when wind speed remains constant, an increase in ice layer thickness leads to an amplified dynamic response.

2) The displacement responses at the cross-arms of towers typically exceed those observed at the tower's apex.

3) The sensitivity of the wind attack angle at $\theta = 0^{\circ}$ and $\theta = 60^{\circ}$ is notably higher.

4) As the thickness of ice accretion and wind speed escalates, their combined influence on the tower-line system progressively intensifies. Consequently, it is advisable to modify the coefficient for this coupling effect during the design of ice-covered lines to bolster the overall reliability of the line.

ACKNOWLEDGMENT

This work was supported by the National Natural Science Foundation of China (52107075), the Fundamental Research Funds for the Central Universities (2572024AW10).

REFERENCES

[1] K. Wu, B. Yan, H. Yang, J. Lu, Z. Xue, M. Liang, and Y. Teng, "Dynamic response characteristics of isolated-span transmission lines after ice-shedding," *IEEE Transactions on Power Delivery*, vol. 38, no. 5, pp. 3519–3530, 2023.

[2] B. Yan, K. Chen, Y. Guo, M. Liang, and Q. Yuan, "Numerical simulation study on jump height of iced transmission lines after ice shedding," *IEEE Transactions on Power Delivery*, vol. 28, no. 1, pp. 216–225, 2013.

[3] L. Yang, Y. Chen, L. Mei, Y. Hao, L. Li, H. Huang, Y. Zhang, L. Zhang, and L. Yang, "Prediction method for response characteristics parameters of isolated-span overhead lines after ice-shedding based on finite element simulation and machine learning," *Electric Power Systems Research*, vol. 229, 2024.

[4] G. Huang, B. Yan, Y. Guo, B. Zhang, and G. Wu, "Experimental study on dynamic response characteristics of isolated-span transmission lines after ice-shedding," *High Voltage*, vol. 8, no. 1, pp. 196–208, 2023.

[5] K. Wu, B. Yan, H. Yang, Q. Liu, J. Lu, and M. Liang, "Characteristics of multi-span transmission lines following ice-shedding," *Cold Regions Science and Technology*, vol. 218, 2024.

[6] R. Pan, C. Liu, J. Liu, Z. Zheng, S. Jiang, Y. Sun, and W. Huang, "Dynamic response and reliability analysis of saddle membrane structures under wind-driven rain load," *Journal of Vibration and Shock*, vol. 42, no. 11, pp. 295–303,323, 2023.

[7] R. Bian, Q. Xu, E. Yu, M. Huang, W. Lou, W. Hu, and L. Zhang, "Multi-variate state monitoring and wind bias reliability analysis of a transmission tower-line system under action of typhoon," *Journal of Vibration and Shock*, vol. 39, no. 3, pp. 52–59, 2020.

[8] Y. Zhang, W. Lou, Z. Chen, L. Wang, and R. Bian, "Aerodynamic force characteristics and wind-induced swing response analysis of ellipse iced conductor with ice bridge," *Journal of South China University of Technology. Natural Science Edition*, vol. 49, no. 7, pp. 125–133, 2021.

[9] X. Dong, M. Zhao, M. Li, and Y. Zhu, "Study on the bouncing process induced by ice shedding on overhead conductors under strong wind conditions," *Applied Sciences-Basel*, vol. 14, no. 10, 2024.

[10] H. Pan, F. Zhou, Y. Ma, Y. Ma, P. Qiu, and J. Guo, "Multiple factors coupling probability calculation model of transmission line ice-shedding," *Energies*, vol. 17, no. 5, 2024.

[11] M. Zhang, Y. Liu, H. Liu, and G. Zhao, "Dynamic response of an overhead transmission tower–line system to high-speed train-induced wind," *Wind and Structures*, vol. 34, no. 4, pp. 335–353, 2022.

[12] L. Tian, J. Luo, M. Zhou, W. Bi, and Y. Liu, "Research on vibration control of a transmission tower-line system using sma-btmd subjected to wind load," *Structural Engineering and Mechanics*, vol. 82, pp. 571–585, 2022.

[13] W. Lou, Y. Zhang, H. Xu, and M. Huang, "Jump height of an iced transmission conductor considering joint action of ice-shedding and wind," *Cold Regions Science and Technology*, vol. 199, p. 103576, 2022.

[14] B. Huo, X. Liu, and S. Yang, "Galloping of iced transmission lines considering multi-torsional modes and experimental validation on a continuous model," *IEEE Transactions on Power Delivery*, vol. 37, no. 4, pp. 3016–3026, 2022.

[15] B. Yan, J. Sheng, K. Jiang, Y. Qi, B. Zhao, and Z. Gong, "Dynamic stability of cathead transmission towers under ice cover and wind loads," *Science Technology and Engineering*, vol. 21, no. 26, pp. 11 166–11 175, 2021.

[16] Q. Xie and L. Sun, "Failure mechanism and retrofitting strategy of transmission tower structures under ice load," *Journal of Constructional Steel Research*, vol. 74, pp. 26–36, 2012.

[17] M. Zhao, B. He, W. Feng, Y. Wang, L. Feng, and C. Wang, "Influence of coupling factors on mechanical property of high voltage transmission tower-line structure under ice loading," *Proceedings of the CSEE*, vol. 38, no. 24, pp. 7141–7148, 2018.

[18] H. Zheng and J. Fan, "Progressive collapse analysis of a truss transmission tower-line system subjected to downburst loading," *Journal Of Constructional Steel Research*, vol. 188, 2022.